5546 *Inorg. Chem.* **2010**, *49*, 5546–5553
DOI: 10.1021/ic1004853

Inorganic Chemistry
Article

Prediction of Reliable Metal−PH_3 Bond Energies for Ni, Pd, and Pt in the 0 and +2 Oxidation States

Raluca Craciun, Andrew J. Vincent, Kevin H. Shaughnessy, and David A. Dixon*

Department of Chemistry, The University of Alabama, Shelby Hall, Box 870336, Tuscaloosa, Alabama 35487-0336

Received March 13, 2010

Phosphine-based catalysts play an important role in many metal-catalyzed carbon−carbon bond formation reactions yet reliable values of their bond energies are not available. We have been studying homogeneous catalysts consisting of a phosphine bonded to a Pt, Pd, or Ni. High level electronic structure calculations at the CCSD(T)/complete basis set level were used to predict the M−PH_3 bond energy (BE) for the 0 and +2 oxidation states for M=Ni, Pd, and Pt. The calculated bond energies can then be used, for example, in the design of new catalyst systems. A wide range of exchange-correlation functionals were also evaluated to assess the performance of density functional theory (DFT) for these important bond energies. None of the DFT functionals were able to predict all of the M−PH_3 bond energies to within 5 kcal/mol, and the best functionals were generalized gradient approximation functionals in contrast to the usual hybrid functionals often employed for main group thermochemistry.

Introduction

Cross-coupling reactions are powerful synthetic methods to form new C−C or C−heteroatom bonds. Although other metals such as nickel, copper, and iron have been successfully used in cross-coupling reactions, palladium[1] remains the most widely used metal in these reactions because of the generally high activity of palladium complexes for a wide range of substrates. It is generally accepted that the main steps[2] involved in the homogeneous palladium catalyzed cross-coupling reactions are as follows: (1) dissociation of supporting ligands to provide the coordinatively unsaturated active species, (2) oxidative addition of the electrophilic substrate, (3) ligand substitution by the nucleophilic reagent, and (4) reductive elimination to give the desired product and regenerate the active species (see Figure S1, Supporting Information). The active $PdL_n(0)$ species can be generated in situ by the reduction of Pd(II) sources in the presence of the supporting ligands. Supporting ligands play a critical role in catalyst activity as they solubilize the metal center, stabilize the Pd(0)/Pd(II) active species, and can promote the oxidative addition step.

Phosphine ligands are a popular choice for use in tailoring the catalytic reactivity of the transition metal complexes. Triarylphosphines were the first ligands used in palladium-catalyzed cross-coupling reactions and are still commonly used. Over the past decade, sterically demanding, electron rich phosphines have been shown, however, to provide highly active catalysts for a wide range of metal-catalyzed cross-coupling reactions.[3,4] These sterically demanding ligands form stable 14-electron $L_2Pd(0)$ species that serve as the catalyst resting state in cross-coupling reactions. Critical species in the catalytic cycle are believed to be monophosphine complexes.[5] Mechanistic studies have shown that ligand dissociation occurs during the oxidative addition step by both dissociative and associative mechanisms depending on the aryl halide substrate.[6−9] A computational study at the density functional theory (DFT)[10] level with the PBE[11] functional and a polarized double-ζ basis set showed that oxidative addition to the LPd(0) species occurred with a lower barrier than for the $L_2Pd(0)$ complex.[12] These authors also showed that the bond dissociation energy (BDE) of the ligand was a good predictor of the rate of oxidative addition

*To whom correspondence should be addressed. E-mail: dadixon@bama.ua.edu.

(1) Tsuji, J. *Synthesis* **1990**, *9*, 739–740.
(2) Crabtree, R. H. *The Organometallic Chemistry of the Transition Metals*; John Wiley and Sons: New York, 2005.
(3) Fu, G. C. *Acc. Chem. Res.* **2008**, *41*, 1555.
(4) Fleckenstein, C. A.; Plenio, H. *Chem. Soc. Rev.* **2010**, *39*, 694.
(5) Christmann, U.; Vilar, R. *Angew. Chem., Int. Ed.* **2005**, *44*, 366.
(6) Stambuli, J. P.; Incarvito, C. D.; Bühl, M.; Hartwig, J. F. *J. Am. Chem. Soc.* **2004**, *126*, 1184.
(7) Galardon, E.; Ramdeehul, S.; Brown, J. M.; Cowley, A.; Hii, K. K.; Jutand, A. *Angew. Chem., Int. Ed.* **2002**, *41*, 1760.
(8) Barrios-Landeros, F.; Hartwig, J. F. *J. Am. Chem. Soc.* **2005**, *127*, 6944.
(9) Barrios-Landeros, F.; Carrow, B. P.; Hartwig, J. F. *J. Am. Chem. Soc.* **2009**, *131*, 8141.
(10) Parr, R. G.; Yang, M. *Density-Functional Theory of Atoms and Molecules*; Oxford University Press: New York, 1989.
(11) (a) Perdew, J. P.; Burke, K.; Ernzerhof, M. *Phys. Rev. Lett.* **1996**, *77*, 3865. (b) Perdew, J. P.; Burke, K.; Ernzerhof, M. *Phys. Rev. Lett.* **1997**, *78*, 1396.
(12) Li, Z.; Fu, Y.; Guo, Q.-X.; Liu, L. *Organometallics* **2008**, *27*, 4043.

 Published on Web 05/03/2010

of aryl chlorides. We had previously used DFT to model the gas-phase Pd−L BDEs for a series of sterically demanding phosphine ligands and showed that there is a correlation between the catalyst activity and BDE.[13,14] We have also shown that the Pd−P BDEs are strongly dependent on the choice of exchange-correlation functional.[15] Since the cleavage of the metal−phosphorus bond is a key step in the catalytic mechanism, it is important to be able to predict such BDEs.

A variety of computational methods have been used to predict the M−L bond energies of different complexes $L-MR_2$ (M = transition metal, R = additional ligand): L = C_2H_2, M = Ni, and R = PR'_3 (R′ = H, CH_3, F, CF_3, C_6H_5);[16] L = olefin, M = Pt, and R = PH_3;[17] L = O_2, C_2H_4 C_2H_2; M = Ni, Pd, Pt, and R = PH_3;[18,19] L = C_{60}, $C_{20}H_{10}$, and $C_{21}H_{12}$; M = Pd, Pt, and R = PH_3;[20] L = SiH_3X (X = H, CH_3, SiH_3), M = Pd, and R = PH_3;[21] L = organostannanes, M = Pd, and R = PH_3, PMe_3;[22] and L = alkyl, M = Ni, Pd, and R = olefins, CO, PH_3, H_2O, Cl.[23,24] The metal phosphine bond dissociation energies for M = Cr, Ni, Mo, and Ru have been investigated at the DFT level with various exchange-correlation functionals.[25]

Despite the importance of the $M-PR_3$ bond, there is not a consistent set of metal phosphine BDEs available which can be used for different Group 10 metals in the important catalytic oxidation states. Our goal is to provide reliable bond energies for the simplest ligand so that more approximate methods can be used, for example, with isodesmic reaction schemes,[26] to predict bond energies for phosphines of practical interest. We describe the results of high level electronic structure calculations at the coupled cluster theory with single and double excitations plus a perturbative triples correction (CCSD(T))[27−30] level with correlation-consistent basis sets extrapolated to the complete basis set limit of the binding energy of the Group 10 transition metals Ni, Pd, and Pt in the 0 and +2 oxidation states to the simplest tertiary phosphorus ligand PH_3 in reactions 1 to 4.

$$MPH_3 \rightarrow M + PH_3 \quad (1)$$

$$M(PH_3)_2 \rightarrow MPH_3 + PH_3 \quad (2)$$

$$MPH_3Cl_2 \rightarrow MCl_2 + PH_3 \quad (3)$$

$$M(PH_3)_2Cl_2 \rightarrow MPH_3Cl_2 + PH_3 \quad (4)$$

These bond energy calculations follow the procedures we have developed for the reliable prediction of a wide range of thermodynamic properties.[31] An advantage of this method is that the extrapolation to the complete basis set limit eliminates the need to consider basis set superposition error (BSSE) as there is no BSSE at the limit. We also report on the ability of a wide range of DFT exchange-correlation functionals to predict these bond energies.

Computational Methods

Equilibrium geometries (Table 2) and vibrational frequencies (Table 3 for stretching frequencies) were calculated first at the DFT level with a range of local,[32,33] gradient-corrected[11,34−44] and hybrid exchange-correlation[11,45−52] functionals (See Table 1 for a list of functionals). The DFT calculations were performed with the augmented correlation consistent double-ζ (aug-cc-pVDZ) basis set for H,[53] P,[54]

(13) DeVasher, R. B.; Spruell, J. M.; Dixon, D. A.; Broker, G. A.; Griffin, S. T.; Rogers, R. D.; Shaughnessy, K. H. *Organometallics* **2005**, *24*, 962.
(14) Hill, L. L.; Smith, J. M.; Brown, W. S.; Moore, L. R.; Guevera, P.; Pair, E. S.; Porter, J.; Chou, J.; Wolterman, C. J.; Craciun, R.; Dixon, D. A.; Shaughnessy, K. H. *Tetrahedron* **2008**, *64*, 6920.
(15) Hill, L. L.; Moore, L. R.; Huang, R.; Craciun, R.; Vincent, A.; Dixon, D. A.; Chou, J.; Woltermann, C. J.; Shaughnessy, K. H. *J. Org. Chem.* **2006**, *71*, 5117.
(16) Piacenza, M.; Rakow, J.; Hyla-Kryspin, I.; Grimme, S. *Eur. J. Inorg. Chem.* **2006**, 213.
(17) Karhánek, D.; Kačer, P.; Kuzma, M.; Šplichalová, L. *J. Mol. Model.* **2007**, *13*, 1009.
(18) Li, J.; Schreckenbach, G.; Ziegler, T. *Inorg. Chem.* **1995**, *34*, 3245.
(19) Massera, C.; Frenking, G. *Organometallics* **2003**, *22*, 2758.
(20) Kameno, Y.; Ikeda, A.; Nakao, Y.; Sato, H.; Sakaki, S. *J. Phys. Chem.A* **2005**, *109*, 8055.
(21) Sakaki, S.; Ogawa, M.; Musashi, Y.; Arai, T. *Inorg. Chem.* **1994**, *33*, 1660.
(22) Ariafard, A.; Lin, Z.; Fairlamb, J. S. *Organometallics* **2006**, *25*, 5788.
(23) Blomberg, M. R. A.; Brandemark, U. B.; Siegbahn, P. E. M.; Mathisen, K. B.; Karlstrom, G. *J. Phys. Chem.* **1985**, *89*, 2171.
(24) Blomberg, M. R. A.; Schule, J.; Siegbahn, P. E. M. *J. Am. Chem. Soc.* **1989**, *111*, 6156.
(25) Minekov, Y.; Occhipinti, G.; Jensen, V. R. *J. Phys. Chem. A* **2009**, *113*, 11833.
(26) Hehre, W. J.; Radom, L.; Schleyer, P. V. R.; Pople, J. A. *Ab Initio Molecular Orbital Theory*; Wiley-Interscience: New York, 1986.
(27) Purvis, G. D., III; Bartlett, R. J. *J. Chem. Phys.* **1982**, *76*, 1910.
(28) Raghavachari, K.; Truck, G. W.; Pople, J. A.; Head-Gordon, M. *Chem. Phys. Lett.* **1989**, *157*, 479.
(29) Watts, J. D.; Gauss, J.; Bartlett, R. J. *J. Chem.. Phys.* **1993**, *98*, 8718.
(30) Bartlett, R. J.; Musial, M. *Rev. Mod. Phys.* **2007**, *79*, 291.
(31) (a) Feller, D.; Dixon, D. A. *J. Phys. Chem. A* **2000**, *104*, 3048. (b) Feller, D.; Dixon, D. A. *J. Chem. Phys.* **2001**, *115*, 3484. (c) Dixon, D. A.; Feller, D.; Peterson, K. A. *J. Chem. Phys.* **2001**, *115*, 2576. (d) Ruscic, B.; Wagner, A. F.; Harding, L. B.; Asher, R. L.; Feller, D.; Dixon, D. A.; Peterson, K. A.; Song, Y.; Qian, X.; Ng, C.; Liu, J.; Chen, W.; Schwenke, D. W. *J. Phys. Chem. A* **2002**, *106*, 2727. (e) Feller, D.; Dixon, D. A. *J. Phys. Chem. A* **2003**, *107*, 9641. (f) Pollack, L.; Windus, T. L.; de Jong, W. A.; Dixon, D. A. *J. Phys. Chem. A* **2005**, *109*, 6934. (g) Feller, D.; Peterson, K. A.; Dixon, D. A. *J. Chem. Phys.* **2008**, *129*, 204015. (h) Dixon, D. A.; Grant, D. J.; Christe, K. O.; Peterson, K. A. *Inorg. Chem.* **2008**, *47*, 5485. (i) Dixon, D. A.; de Jong, W. A.; Peterson, K. A.; Christe, K. O.; Schrobilgen, G. J. *J. Am. Chem. Soc.* **2005**, *127*, 8627. (j) Dixon, D. A.; Grant, D. J.; Peterson, K. A.; Christe, K. O.; Schrobilgen, G. J. *Inorg. Chem.* **2008**, *47*, 5485.
(32) Slater, J. C. *Quantum Theory of Molecules and Solids*; McGraw-Hill: New York, 1974; Vol. *4*.
(33) Vosko, S. H.; Wilk, L.; Nusair, M. *Can. J. Phys* **1980**, *58*, 1200.
(34) Becke, A. D. *Phys. Rev. A* **1988**, *38*, 3098.
(35) Lee, C.; Yang, W.; Parr, R. G. *Phys. Rev. B* **1988**, *37*, 785.
(36) Perdew, J. P. *Phys. Rev. B* **1986**, *33*, 8822.
(37) Burke, K.; Perdew, J. P. Wang., Y. In *Electronic Density Functional Thoery: Recent Progress and New Directions*; Dobson, J. F., Vignale, G., Das, M. P., Eds.; Plenum: New York, 1998; p 81.
(38) Becke, A. D. *J. Chem. Phys.* **1996**, *104*, 1040.
(39) Perdew, J. P.; Wang, Y. *Phys. Rev. B* **1991**, *45*, 13244.
(40) Adamo, C.; Barone, V. *J. Chem. Phys.* **1998**, *108*, 664.
(41) Handy, N. C.; Cohen, A. J. *Mol. Phys.* **2001**, *99*, 403.
(42) Tao, J. M.; Perdew, J. P.; Staroverov, V. N.; Scuseria, G. E. *Phys. Rev. Lett.* **2003**, *91*, 146401.
(43) Van Voorhis, T.; Scuseria, G. E. *J. Chem. Phys.* **1998**, *109*, 400.
(44) Hamprecht, F. A.; Cohen, A. J.; Tozer, D. J.; Handy, N. C. *J. Chem. Phys.* **1998**, *109*, 6264.
(45) Becke, A. D. *J. Chem. Phys.* **1993**, *98*, 5648.
(46) Becke, A. D. *J. Chem. Phys.* **1996**, *104*, 1040.
(47) Adamo, C.; Barone, V. *Chem. Phys. Lett.* **1997**, *274*, 242.
(48) Hamprecht, F. A.; Cohen, A.; Tozer, D. J.; Handy, N. C. *J. Chem. Phys.* **1998**, *109*, 6264.
(49) Wilson, P. J.; Bradley, T. J.; Tozer, D. J. *J. Chem. Phys.* **2001**, *115*, 9233.
(50) Schmider, H. L.; Becke, A. D. *J. Chem. Phys.* **1998**, *108*, 9624.
(51) Boese, A. D.; Martin, J. M. L. *J. Chem. Phys.* **2004**, *121*, 3405.
(52) Tao, J. M.; Perdew, J. P.; Staroverov, V. N.; Scuseria, G. E. *Phys. Rev. Lett.* **2003**, *91*, 146401.
(53) Dunning, T. H., Jr. *J. Chem. Phys.* **1989**, *90*, 1007.

Table 1. Benchmarked DFT Exchange-Correlation Functionals

functional	exchange	correlation	type	refs.
SVWN5	Slater	VWN5	LSDA	32, 33
BLYP	Becke 88	Lee−Yang−Parr	GGA	34, 35
BP86	Becke 88	Perdew 86	GGA	34, 36
BPW91	Becke 88	Perdew−Wang 91	GGA	34, 37
BB95	Becke 88	Becke 95	GGA	34, 38
PW91	Perdew−Wang 91	Perdew−Wang 91	GGA	39, 37
mPWPW91	Adamo and Barone's modified PW91	Perdew−Wang 91	GGA	40, 37
PBE	Perdew−Burke−Ernzerhof	Perdew−Burke−Ernzerhof	GGA	11
OLYP	Handy's OPTX	Lee−Yang−Parr	GGA	41, 35
TPSS	Tao−Perdew−Staroverov−Scuseria	Tao−Perdew−Staroverov−Scuseria	GGA	42
VSXC	van Voorhis −Scuseria	van Voorhis −Scuseria	GGA	43
HCTH	Handy	Handy	GGA	44
B3LYP	Becke 93	Lee−Yang−Parr	HGGA	45, 35
B3P86	Becke 93	Perdew 86	HGGA	45, 36
B3PW91	Becke 93	Perdew−Wang 91	HGGA	45, 37
B1B95	Becke 96	Becke 95	HGGA	46, 38
B1LYP	Becke 96	Lee−Yang−Parr	HGGA	46, 35
mPW1	Barone's modified PW91	Perdew−Wang 91	HGGA	47, 39, 37
B971	Handy−Tozer's modified B97	Handy−Tozer's modified B97	HGGA	48
B972	Wilson−Bradley−Tozer's modified B97	Wilson−Bradley−Tozer's modified B97	HGGA	49
B98	Becke 98	Becke 98	HGGA	50
PBE1	Perdew−Burke−Ernzerhof	Perdew−Burke−Ernzerhof	HGGA	11
O3LYP	Handy's OPTX	Lee−Yang−Parr	HGGA	41, 35
BMK	Boese −Martin	Boese −Martin	HGGA	51
TPSSh	Tao−Perdew−Staroverov−Scuseria	Tao−Perdew−Staroverov−Scuseria	HGGA	52

Table 2. MPH_3, $M(PH_3)_2$, MPH_3Cl_2, and $M(PH_3)_2Cl_2$ Optimized M−P and M−Cl Bond Lengths (Å) at the B3LYP and CCSD(T) Levels

		M−P (Å)			M−Cl (Å)		
M	reactant state/sym	B3LYP/aD-PP	CCSD(T)/ aD-PP	CCSD(T)/ aT-PP	B3LYP/aD-PP	CCSD(T)/ aD-PP	CCSD(T)/ aT-PP
			Reactant = MPH_3				
Ni	$^1A_1/C_{3v}$	2.025	1.998				
Pd	$^1A_1/C_{3v}$	2.202	2.175	2.144			
Pt	$^1A_1/C_{3v}$	2.131	2.102	2.089			
			Reactant = $M(PH_3)_2$				
Ni	$^1A_1'/D_{3h}$	2.124	2.109	2.090			
Pd	$^1A_1'/D_{3h}$	2.291	2.272	2.250			
Pt	$^1A_1'/D_{3h}$		2.244	2.222			
			Reactant = MPH_3Cl_2				
Ni	$^1A'/C_s$	2.129	2.154	2.062	2.113	2.250	2.080
					2.124	2.245	2.095
Pd	$^1A'/C_s$	2.196	2.162	2.132	2.284	2.281	2.249
					2.297	2.266	2.266
Pt	$^1A'/C_s$	2.168	2.134	2.114	2.296	2.276	2.259
					2.310	2.290	2.276
			Reactant = $M(PH_3)_2Cl_2$				
Ni	$^1A_g/C_{2h}$	2.234	2.202	2.152	2.189	2.174	2.178
Pd	$^1A_g/C_{2h}$	2.327	2.301	2.280	2.335	2.309	2.912
Pt	$^1A_g/C_{2h}$	2.312	2.277	2.270	2.353	2.336	2.309

and Cl[54] and the aug-cc-pVDZ-PP basis sets with accompanying small-core relativistic pseudopotentials for the transition metal atoms;[55−57] we label the combined basis set as aN-PP with N = D, T, Q. The B3LYP geometries were used as a starting point for optimizations at the CCSD(T) level. For P and Cl, we have used the aug-cc-pV(n+d)Z basis sets[58] in the CCSD(T) calculations with n = D and T for the geometry optimizations. The aug-cc-pV(T+d)Z geometries were used for single point aug-cc-pV(Q+d)Z calculations. The CCSD(T) energies were extrapolated to the complete basis set (CBS) limit by using a mixed Gaussian/exponential formula.[59] The bond energy is given as

$$\mathrm{BDE} = E(\mathrm{MR}_x\mathrm{L}_n) - E(\mathrm{L}) - E(\mathrm{MR}_x\mathrm{L}_{n-1}) \qquad (5)$$

(54) Woon, D. E.; Dunning, T. H., Jr. *J. Chem. Phys.* **1993**, *98*, 1358.
(55) Figgen, D.; Peterson, K. A.; Dolg, M.; Stoll, H. *J. Chem. Phys.* **2009**, *130*, 164108. Spohn, B.; Goll, E.; Stoll; Figgen, D.; Peterson, K. A. *J. Phys. Chem. A* **2009**, *113*, 12478.
(56) Peterson, K. A.; Figgen, D.; Dolg, M.; Stoll, H. *J. Chem. Phys.* **2007**, *126*, 124101. Peterson, K. A.; Figgen, D.; Stoll, H. *J. Chem. Phys.* **2008**, *128*, 034110.
(57) (a) Balabanov, N. B.; Peterson, K. A. *J. Chem. Phys.* **2005**, *123*, 064107. (b) Balabanov, N. B.; Peterson, K. A. *J. Chem. Phys.* **2006**, *125*, 074110.
(58) Dunning, T. H., Jr.; Peterson, K. A.; Wilson, A. K. *J. Chem. Phys.* **2001**, *114*, 9244.
(59) Peterson, K. A.; Woon, D. E.; Dunning, T. H., Jr. *J. Chem. Phys.* **1994**, *100*, 7410.

Table 3. M−P and M−Cl Stretching Frequencies (cm^{-1}) and IR Intensities (km/mol) in parentheses at the B3LYP/aD-PP Level

M	reactant state/ sym	M−P stretching freq	M−Cl stretching freq
		Reactant = MPH_3	
Ni	$^1A_1/C_{3v}$	437(29)	
Pd	$^1A_1/C_{3v}$	352(11)	
Pt	$^1A_1/C_{3v}$	446(13)	
		Reactant = $M(PH_3)_2$	
		Sym A_1'	**Asym A_2''**
Ni	$^1A_1'/D_{3h}$	325(0)	377(135)
Pd	$^1A_1'/D_{3h}$	295(0)	295(73)
Pt	$^1A_1'/D_{3h}$	364(0)	313(59)
		Reactant = MPH_3Cl_2	
			Sym **Asym**
Ni	$^1A'/C_s$	394(3)	331(3) 449(98)
Pd	$^1A'/C_s$	385(13)	321(1) 369(78)
Pt	$^1A'/C_s$	436(24)	357(73) 344(9)
		Reactant = $M(PH_3)_2Cl_2$	
		Sym A_g	**Asym B_u** **Sym A_g** **Asym B_u**
Ni	$^1A_g/C_{2h}$	267(0)	334(3) 302(0) 400(49)
Pd	$^1A_g/C_{2h}$	290(0); 305(0)[a]	283(0) 290(0); 305(0)[a] 348(52)
Pt	$^1A_g/C_{2h}$	345(0)	282(3) 319(0) 333(51)

[a] The Pd−P and Pd−Cl sym stretches for $Pd(PH_3)_2Cl_2$ are coupled and the values of 290 and 305 cm^{-1} are not readily assigned.

Several additional corrections have been used to adjust the CBS valence electronic energies: (1) a core−valence correlation correction (ΔE_{CV}) calculated at the CCSD(T) level with the aug-cc-pwCVTZ basis set[54] for P and Cl and the aug-cc-pwCVTZ-PP basis set[55,55−57] for the transition metal atoms (denoted as awCVTZ); (2) scalar relativistic corrections on the F atoms and corrections for any errors in the metal pseudopotentials for the binding energies (BDEs). The latter is calculated by taking the difference between the BDE calculated at the Douglas−Kroll−Hess[60] level with the CCSD(T)-DK method and the aT-DK basis set[55,61,62] and the BDE calculated at the CCSD(T)/aT-PP level (eq 6); and

$$\Delta BDE_{Rel} = BDE(CCSD(T)\text{-}DK/aT\text{-}DK) - BDE(CCSD(T)/at\text{-}PP) \quad (6)$$

(3) the zero point energy calculated at the DFT level with aug-cc-pVDZ and aug-cc-pVDZ-PP basis sets. The bond dissociation energy is calculated as the sum of the different contributions (eq 7).

$$BDE_{0K} = BDE_{CBS} + \Delta BDE_{ZPE} + \Delta BDE_{CV} + \Delta BDE_{Rel} \quad (7)$$

The T_1 diagnostics[63] are given in the Supporting Information. As expected, the values are largest for the Ni compounds suggesting the most multireference character in these molecules. The largest T_1 values for the Pd and Pt compounds are for the triplet MCl_2 with the other values under 0.03 consistent with minimal multireference character in the starting wave function.

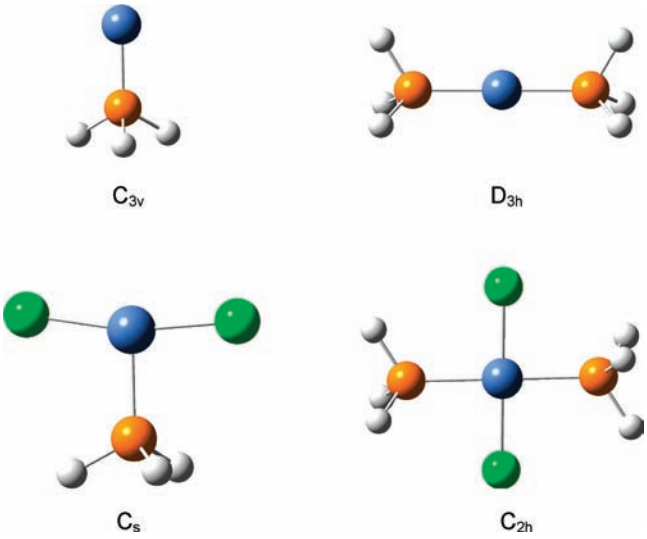

Figure 1. MPH_3, $M(PH_3)_2$, MPH_3Cl_2, and $M(PH_3)_2Cl_2$ structures calculated at the B3LYP/aug-cc-pVDZ-PP level.

The DFT calculations were done with the Gaussian program system[64] and the CCSD(T) calculations with the Molpro program system[65] on computers at The University of Alabama, the Alabama Supercomputing Center, and the Molecular Sciences Computing Facility in the William R. Wiley Environmental Molecular Sciences Laboratory at the Pacific Northwest National Laboratory.

Results and Discussion

Geometries and Vibrational Frequencies. Schematics of the ground state geometries of the 4 possible complexes are given in Figure 1.

MPH_3. All structures were optimized as singlet states of C_{3v} symmetry. At the B3LYP/aD-PP level, the triplet states of $NiPH_3$ and $PtPH_3$ are 1.8 and 42.8 kcal/mol, respectively, higher in energy than the singlet. The energy of the triplet state of $NiPH_3$ was evaluated at higher levels, and, at the CCSD(T)/CBS level, it was found to be 17.2 kcal/mol higher in energy than the singlet state. The M−P bond distance increases from Ni to Pd and then decreases slightly for Pt. Our calculated CCSD(T)

(60) (a) Douglas, M.; Kroll, N. M. *Ann. Phys.* **1974**, *82*, 89. (b) Hess, B. A. *Phys. Rev. A.* **1985**, *32*, 756. (c) Hess, B. A. *Phys. Rev. A.* **1986**, *33*, 3742.
(61) de Jong, W. A.; Harrison, R. J.; Dixon, D. A. *J. Chem. Phys.* **2001**, *114*, 48.
(62) EMSL basis set library. http://www.emsl.pnl.gov/forms/basisform.html
(63) Lee, T. J.; Taylor, P. R. *Int. J. Quantum Chem.* **1989**, *S23*, 199.
(64) Frisch, M. J.; Trucks, G. W.; Schlegel, H. B.; Scuseria, G. E.; Robb, M. A.; Cheeseman, J. R.; Montgomery, Jr., J. A.; Vreven, T.; Kudin, K. N.; Burant, J. C.; Millam, J. M.; Iyengar, S. S.; Tomasi, J.; Barone, V.; Mennucci, B.; Cossi, M.; Scalmani, G.; Rega, N.; Petersson, G. A.; Nakatsuji, H.; Hada, M.; Ehara, M.; Toyota, K.; Fukuda, R.; Hasegawa, J.; Ishida, M.; Nakajima, T.; Honda, Y.; Kitao, O.; Nakai, H.; Klene, M.; Li, X.; Knox, J. E.; Hratchian, H. P.; Cross, J. B.; Bakken, V.; Adamo, C.; Jaramillo, J.; Gomperts, R.; Stratmann, R. E.; Yazyev, O.; Austin, A. J.; Cammi, R.; Pomelli, C.; Ochterski, J. W.; Ayala, P. Y.; Morokuma, K.; Voth, G. A.; Salvador, P.; Dannenberg, J. J.; Zakrzewski, V. G.; Dapprich, S.; Daniels, A. D.; Strain, M. C.; Farkas, O.; Malick, D. K.; Rabuck, A. D.; Raghavachari, K.; Foresman, J. B.; Ortiz, J. V.; Cui, Q.; Baboul, A. G.; Clifford, S.; Cioslowski, J.; Stefanov, B. B.; Liu, G.; Liashenko, A.; Piskorz, P.; Komaromi, I.; Martin, R. L.; Fox, D. J.; Keith, T.; Al-Laham, M. A.; Peng, C. Y.; Nanayakkara, A.; Challacombe, M.; Gill, P. M. W.; Johnson, B.; Chen, W.; Wong, M. W.; Gonzalez, C.; and Pople, J. A. *Gaussian 03*, Revision E.01; Gaussian, Inc.: Wallingford, CT, 2004.
(65) Werner, H.-J.; Knowles, P. J.; Lindh, R.; Manby, F. R.; Schütz, M.; Celani, P.; Korona, T.; Rauhut, G.; Amos, R. D.; Bernhardsson, A.; Berning, A.; Cooper, D. L.; Deegan, M. J. O.; Dobbyn, A. J.; Eckert, F.; Hampel C.; Hetzer, G.; Lloyd, A. W.; McNicholas, S. J.; Meyer W.; Mura, M. E.; Nicklass, A.; Palmieri, P.; Pitzer, R.; Schumann, U.; Stoll, H.; Stone, A. J.; Tarroni, R.; Thorsteinsson, T. *MOLPRO, version 2008.1, a package of ab initio programs*; See http://www.molpro.net.

values for the M−P bond distances are as follows: 1.998 Å for M = Ni (aD-PP), 2.144 Å Å for M = Pd (aT-PP level), and 2.089 Å for M = Pt (aT-PP level). At the CI level with a modest basis set, the Ni−P bond distance is predicted to be 2.196 Å and the Pd−P bond distance is predicted to be 2.355 Å.[24]

$M(PH_3)_2$. The ground state structure for all three metals studied, Ni, Pd, and Pt was found to be a singlet state with a linear geometry and D_{3h} symmetry. Our calculated Ni−P bond distance is 2.090 Å (CCSD(T)/aT-PP). A comparable calculated bond distance of 2.084 Å for the C_{2v} bent structure of $Ni(PH_3)_2$ at the BP86/TZV(2df,2pd) level has been reported[16] and a longer value of 2.249 Å at the CI level was reported.[23] Calculations[18,19] at the BP86/TZV and B3LYP/LANL2DZ levels have predicted $Ni(PH_3)_2$ to be linear. For Pd−P, our calculated CCSD(T)/aT-PP bond distance is 2.250 Å. A linear structure for $Pd(PH_3)_2$ with a Pd−P bond distance of 2.408 Å was also predicted[21] at the MP4 level.

MCl_2. Geometries have been optimized for both singlet and triplet states. The linear $NiCl_2$ triplet is lower in energy by 31.5 kcal/mol than the singlet bent C_{2v} structure at the CCSD(T)/CBS level. For $PdCl_2$ and $PtCl_2$, the linear triplet structures are also more stable than the singlet structures by 6.1 and 10.3 kcal/mol, respectively.

We investigated the singlet−triplet splitting of MCl_2 as a function of the molecular orbital-based method (Hartree−Fock (HF), spin restricted second order Møller−Plesset (MP2),[66,67] CCSD and CCSD(T)) with the aug-cc-pVTZ-PP basis set (see Supporting Information). The calculated values show that there is a large variation in the method and the variation is molecule dependent. For $NiCl_2$, the HF (spin restricted) value is far from the CCSD(T) value (too large by 39 kcal/mol) and the MP2 value differs from the CCSD(T) value by 11 kcal/mol. The CCSD value is still too large by 7 kcal/mol as compared to the CCSD(T) value. The agreement of the lower level methods with CCSD(T) improves for $PdCl_2$ which has the smallest singlet−triplet splitting. The CCSD value is within 1 kcal/mol of the CCSD(T) value and even the HF value is in good agreement. The largest error is found for the MP2 value. For $PtCl_2$, the CCSD value is again within 1 kcal/mol of the CCSD(T) value. In this case the HF value is 9 kcal/mol too large and the MP2 value is 7 kcal/mol too small. The fact that the largest errors are found for the first row transition metal atom is consistent with the fact that it is quite difficult to reliably predict the intrashell d correlation energies for the first row transition metal atoms. Thus the reliable prediction of the singlet−triplet splitting in these compounds does require CCSD(T), especially if one wants to compare trends in different rows within a column.

MPH_3Cl_2. All structures were optimized in the singlet state. The $NiPH_3Cl_2$ triplet state is 22.4 kcal/mol higher in energy than the singlet at the CCSD(T)/CBS level. The $PtPH_3Cl_2$ triplet state is 22.5 kcal/mol higher than the singlet at the B3LYP/aD-PP level and was not optimized further with CCSD(T). The M−P bond distance follows the same trend as for $M-PH_3$, increasing from Ni to Pd and then decreasing for Pt. The two M−Cl bond distances are slightly different from each other because of the C_s symmetry of the molecule, and the average value increases from Ni to Pt.

$M(PH_3)_2Cl_2$. The ground states of the dichloro diphosphine metal complexes are also singlets. For M = Ni, the singlet−triplet splitting at the B3LYP/aD-PP level is predicted to be only 2.3 kcal/mol, so CCSD(T) single point calculations have been performed up to the aT-PP level to differentiate between the two possible states. At the CCSD(T)/aT-PP level, the triplet state is higher in energy by 14.1 kcal/mol than the singlet. For M = Pt, the triplet was found to be 44.9 kcal/mol higher than the singlet at the B3LYP/aD-PP level and was not optimized further with CCSD(T). The M−P and M−Cl bond distances follow the same trend as in MPH_3Cl_2 compounds.

The dependence of the singlet−triplet splitting in $Ni(PH_3)_2Cl_2$ on the molecular orbital method is consistent with the results for $NiCl_2$. In this case, the HF splitting is of the wrong sign and in error by 68 kcal/mol. The MP2 value, surprisingly, is within about 1 kcal/mol of the CCSD(T) value, and the CCSD value is 10 kcal/mol too small. For $Pt(PH_3)_2Cl_2$, the singlet−triplet splitting at the HF level is in error by 17 kcal/mol too positive and is too negative by 16 kcal/mol at the MP2 level both compared to the CCSD(T) value. The CCSD value is within 1 kcal/mol of the CCSD(T) value for this molecule with a large singlet−triplet splitting.

Vibrational Frequencies. The M−P and M−Cl stretching frequencies (cm^{-1}) calculated at the B3LYP/aD-PP level are given in Table 3. All M−P frequencies are predicted to be in the range of 300−450 cm^{-1} except for $M(PH_3)_2Cl_2$ compounds where they range from 267 to 345 cm^{-1}. The stretching frequencies values correlate with the bond lengths and are at higher values for shorter bonds.

Bond Dissociation Energies. $M-PH_3$ bond dissociation energies (BDEs) for reactions 1 to 4 have been calculated at different levels of theory with all species in their ground states. The results are in Table 4. For all of the reactions, the zero point energy correction is less than 3 kcal/mol, and the effect is to decrease the BDEs. The core−valence corrections can either increase or decrease the BDEs, but the effect is also small, less than 2 kcal/mol, except for M = Pd in reaction 1 where the ΔE_{CV} is 2.6 kcal/mol. The relativistic corrections are less than 2 kcal/mol except for M = Ni in reaction 1 where ΔE_{Rel} is 4.1 kcal/mol, and can either increase or decrease the BDEs.

Care has to be taken in the prediction of the atomic energies for the prediction of the $M-PH_3$ BDE. For Ni, we calculated the $Ni-PH_3$ BDE of reaction 1 at the CCSD(T)/CBS level relative to the $^1S_0$ excited state of the atom which has no spin orbit correction and corrected the calculated BDE with the experimental energy difference[68] of 42.11 kcal/mol with respect to the $^3F_4$

(66) (a) Møller, C.; Plesset, M. S. *Phys. Rev.* **1934**, *46*, 618. (b) Pople, J. A.; Binkley, J. S.; Seeger, R. *Int. J. Quantum Chem. Symp.* **1976**, *10*, 1.

(67) Lauderdale, W. J.; Stanton, J. F.; Gauss, J.; Watts, J. D.; Bartlett, R. J. *Chem. Phys. Lett.* **1991**, *187*, 21. Amos, R. D.; Andrews, J. S.; Handy, N. C.; Knowles, P. J. *Chem. Phys. Lett.* **1991**, *185*, 256.

(68) Moore, C. E. *Atomic Energy Levels as Derived from the Analysis of Optical Spectra, Vol. 1, H to V*; U.S. National Bureau of Standards Circular 467, COM-72−50282; U.S. Department of Commerce, National Technical Information Service: Washington, DC, 1949.

(69) Craciun, R.; Picone, D.; Long, R. T.; Li, S.; Dixon, D. A.; Peterson, K. A.; Christe, K. O. *Inorg. Chem.* **2010**, *49*, 1056.

(70) Li, S.; Hennigan, J. M.; Dixon, D. A.; Peterson, K. A. *J. Phys. Chem. A* **2009**, *113*, 7861.

Table 4. Components for Calculated M−PH_3 Binding Energy for Reactions 1 to 4 (M = Ni, Pd, Pt)

M	reactant state/sym	metal product state/sym	ΔE_{CBS}	ΔE_{ZPE}	ΔE_{CV}	ΔE_{rel}	BDE
		Reactant = MPH_3					
Ni−P[a]	$^1A_1/C_{3v}$	$^1S_0$	71.81	−1.74	−0.87	−4.10	23.0
Pd−P	$^1A_1/C_{3v}$	$^1S_0$	42.16	−1.69	2.60	−1.23	41.8
Pt−P[a]	$^1A_1/C_{3v}$	$^1S_0$	82.38	−2.27	3.47	−2.12	63.9
		Reactant = $M(PH_3)_2$					
Ni−P	$^1A_1'/D_{3h}$	$^1A_1/C_{3v}$	39.51	−1.69	0.27	1.62	39.7
Pd−P	$^1A_1'/D_{3h}$	$^1A_1/C_{3v}$	33.67	−1.72	1.82	−0.18	33.6
Pt−P	$^1A_1'/D_{3h}$	$^1A_1/C_{3v}$	45.91	−1.90	1.39	0.05	45.5
		Reactant = MPH_3Cl_2					
Ni−P	$^1A'/C_s$	$^3\Sigma_g/D_{\infty h}$	19.52	−2.74	1.67	−1.94	16.5
Pd−P	$^1A'/C_s$	$^3\Sigma_g/D_{\infty h}$	62.15	−2.83	−0.46	−0.46	58.4
Pt−P	$^1A'/C_s$	$^3\Sigma_g/D_{\infty h}$	60.30	−2.83	−1.95	−1.30	54.2
		Reactant = $M(PH_3)_2Cl_2$					
Ni−P	$^1A_g/C_{2h}$	$^1A'/C_s$	26.70	−2.21	0.50	−0.53	24.5
Pd−P	$^1A_g/C_{2h}$	$^1A'/C_s$	32.66	−2.05	1.37	0.14	32.1
Pt−P	$^1A_g/C_{2h}$	$^1A'/C_s$	41.26	−2.24	1.14	0.17	40.3

[a] BDE calculated with respect to the $^1S_0$ excited states of Ni and Pt and corrected with the experimental energy difference of 42.11 and 17.54 kcal/mol, respectively, with respect to the $^3F_4$ ground state of Ni and to the $^3D_3$ ground state of Pt.

ground state. This builds on the approach that we have developed for predicting heats of formation of transition metal compounds.[69−71] The DFT functionals predict the correct wave function for the s^2d^8 triplet state of the Ni atom but not for the d^{10} singlet state where they usually yield the s^1d^9 excited singlet state. To assess the performance of the DFT functionals, we calculated the Ni−PH_3 BDE of reaction 1 relative to the $^3F_4$ ground state at the CCSD(T)/CBS level together with the zero point energy and core−valence corrections and subtracted the experimental J-averaged atomic spin orbit correction of 2.78 kcal/mol. The resulting value was used to compare the Ni−PH_3 BDEs calculated at the DFT level with each of the functionals listed in Table 1. Blomberg et al.[24] predicted that the triplet state of Ni is more stable than the singlet by only 8 kcal/mol at the CI level and noted that the corresponding calculated nickel-ligand binding energies are too small because of the small basis sets used in calculations. For Pd, the d^{10} singlet state is the ground state, so no correction is needed. In calculating the Pt−PH_3 BDE of reaction 1, we used the same approach as for Ni−PH_3, and calculated the Pt−PH_3 BDE in reaction 1 for the $^1S_0$ excited state which was corrected by an energy difference of 17.54 kcal/mol with respect to the $^3D_3$ ground state.

In reactions 1 and 2, the metal is in the 0 oxidation state. The energy to break the first M−PH_3 is largest for Pt and lowest for Pd. A different trend is predicted for the metal in the +2 oxidation state as shown in reaction 4 with the M−PH_3 BDEs increasing from M = Ni to M = Pt. Comparing the BDEs for reactions 2 and 4, we see that the higher oxidation state has the lower BDE with the two BDEs being comparable for Pd within 2 kcal/mol. For reaction 1, the second BDE for $M(PH_3)_2$, the M−PH_3 BDEs increase from M = Ni to M = Pt with that for Pt being almost 40 kcal/mol greater than that for Ni. The second BDE is greater than the first for Pt and Pd and the opposite holds for Ni all in the 0 oxidation state. In reaction 3 where the metal is in the +2 oxidation state, the second BDEs increase from ∼16 kcal/mol for M = Ni to ∼56 kcal/mol for M = Pd and Pt. In the +2 oxidation state, the same trend for the first and second BDEs is found as for the 0 oxidation state.

Blomberg and co-workers[23] investigated the nature of the Ni binding to the H_2O, CO, and PH_3 ligands at the SCF, MCSCF, and CI levels. They predicted for $NiPH_3$ and $Ni(PH_3)_2$ (both singlets) that the binding energies are 13.7 (singlet atom) and 41.0 kcal/mol. The former value is much lower than our value of 72 kcal/mol, and the latter is comparable to our value of 40 kcal/mol. Subsequently, Blomberg et al.[24] studied the interaction of palladium with various ligands including PH_3 and predicted a bond energy of 16 kcal/mol for reaction 1, less than half the BDE predicted by us at a higher level.

A useful comparison is the basis set dependence of the BDEs at the CCSD(T) level. If a smaller basis set can be used for the calculations, this is a clear computational advantage because of the N^7 (N = number of basis functions) scaling of CCSD(T). For $M(PH_3)_2Cl_2$ with the M in the formal +2 oxidation state, the M−P BDE is not strongly basis set dependent with the aug-c-pVDZ-PP results within better than 1.5 kcal/mol of the aug-c-pVQZ-PP results. The basis set effect is larger for M-$(PH_3)_2$ with M in the 0 oxidation state with the aug-cc-pVDZ-PP results within better than 3 kcal/mol of the aug-c-pVQZ-PP results. This basis set dependence is consistent with the fact that the M−P bond in these compounds is an electron pair donor/acceptor type bond.[72] The basis set effects are substantially larger for $M(PH_3)Cl_2$ and $M(PH_3)$ with differences up to ∼8 kcal/mol between the aug-cc-pVDZ-PP and aug-cc-pVQZ basis sets. The vacant binding site leads to a larger basis set effect on the M−PH_3 bond energies.

(71) Li, S.; Dixon, D. A. *J. Phys. Chem. A* **2010**, *114*, 2665.

(72) (a) Dixon, D. A.; Gutowski, M. *J. Phys. Chem. A* **2005**, *109*, 5129. (b) Grant, D. J.; Dixon, D. A. *J. Phys. Chem. A* **2005**, *109*, 10138.

Table 5. Average Deviations of the Metal-Phosphine Bond Dissociation Energies from the CCSD(T) Calculated Values in kcal/mol

functional	Rxn (1)	Rxn (2)	Rxn (3)	Rxn (44)
SVWN5	−24.7	−11.0	−13.2	−9.0
BLYP	8.7	6.3	12.3	8.6
BP86	1.1	1.9	5.4	4.2
BPW91	2.7	3.3	6.9	5.5
BB95	−4.4	3.9	5.8	5.8
PW91	−0.7	0.3	3.2	1.9
mPWPW91	1.2	1.9	5.2	3.8
PBE	−0.3	0.8	3.8	2.6
OLYP	8.8	10.8	12.2	13.0
TPSS	−5.0	2.3	5.8	3.1
VSXC	2.9	3.0	7.3	−0.5
HCTH	−11.9	8.7	9.2	10.4
B3LYP	17.6	6.1	13.7	6.2
B3P86	9.7	2.1	7.2	2.0
B3PW91	12.1	3.9	9.8	3.9
B1B95	12.9	5.0	9.7	3.6
B1LYP	22.4	7.1	16.0	6.7
mPW1PW91	14.3	3.2	9.6	2.4
B971	16.7	4.3	10.8	3.6
B972	11.4	6.1	9.6	5.5
B98	17.6	4.9	11.6	4.2
PBE1PBE	13.0	2.4	8.5	1.4
O3LYP	10.6	9.8	13.1	10.7
BMK	33.1	7.5	16.0	2.4
TPSSh	−5.0	2.0	6.4	2.7

Performance of DFT. The calculated bond energies for each of the four reactions for the functionals in Table 1 are given in the Supporting Information. The average deviations over the three metals from the CCSD(T)/CBS values plus additional corrections are given in Table 5. As expected from our previous studies on the performance of DFT exchange-correlation functionals for the prediction of the thermodynamic properties of transition metal complexes,[69−71] the local functional SVWN5 displays large average deviations, which predicts BDEs up to 44 kcal/mol too large. This is the typical overbinding exhibited by the local approximation. It is important to note that the values in Table 5 are average values, and that the errors in the DFT values are not necessarily the same for each metal.

The GGA functionals perform better than the local functional as would be expected. The predicted average bond energies are smaller than the CCSD(T) values with a few exceptions mostly for reaction 1. The OLYP and HCTH functionals do not work well for these bond energies. However, there is no regular pattern to the discrepancies, and the error is not constant for the different oxidation states, nor is it constant for the reactions 2 and 4, for loss of the first PH_3 or reactions 1 and 3 for loss of the second PH_3. The widely used PW91 and PBE GGA functionals are within 4 kcal/mol of the CCSD(T) values for all four reactions. The largest error for these two functionals is for reaction 3. Thus these functionals could be used for semiquantitative predictions of the metal-phosphine bond energies. However, we note that the sign of the error for the bond energy changes from negative (overbinding) to positive (underbinding) for most of the reactions with these two functionals and that there is an error of more than 10 kcal/mol for MPH_3Cl_2 with each of these functionals for M = Pt so that the values are not even qualitatively correct.

Most of the hybrid GGA functionals do extremely poorly in predicting the metal-phosphine bond energies, including the widely used B3LYP functional. The smallest average bond energy errors were predicted using the TPSSh functional but this functional has errors as large as −13 kcal/mol for reaction 1 with M = Ni and +16 for reaction 3 for M = Pt. The hybrid functionals tend to predict bond energies that are too low, and in some cases the phosphine is predicted to be unbound. This arises from the difficulties that these functionals appear to have for the prediction of the correct state energy differences of the metal atoms or of MCl_2. Again, there is no apparent pattern in the errors except that most functionals seem to do best for the $Pd-PH_3$ bond energies in reactions 1 to 4.

There really is not any functional that works for every metal for all four reactions. DFT can be used to provide qualitative conclusions about these bond energies but it may not work well for the direct comparison of bond energies in a column. An important point of the CCSD(T)/CBS calculations is to provide a set of results against which to test the various DFT functionals. For the set of functionals tested, there is no functional that comes close to chemical accuracy for these types of bond energy predictions which are relevant to the prediction of catalytic cycles. One use for the CCSD(T)/CBS results would be for the development of isodesmic reaction schemes where more reliable bond energies can be developed from reactions like reaction 8 which gives the M−P bond energy of $M(PR_3)_2Cl_2$ relative to that of $M(PH_3)_2Cl_2$.

$$PH_3 + M(PH_3)Cl_2 + M(PR_3)_2Cl_2 \rightarrow M(PH_3)_2Cl_2 + M(PR_3)Cl_2 + PR_3 \quad (8)$$

$$BDE(M(PR_3)_2Cl_2) = \Delta H(\text{Rxn } 8) + BDE(M(PH_3)_2Cl_2) \quad (9)$$

The value for ΔH(Rxn 8) can be calculated at the DFT level with an appropriate functional as most of the effect of the substituent is on the P, and DFT should be able to handle this if the substituents are not too large. Of course, a parametrized functional may exist (and in theory does exist) that does give good agreement with the CCSD(T) results but many of the newest functionals contain a large number of empirical parameters and so become less of a first principles calculation and potentially more susceptible to issues with the parametrization and the data used in the parametrization. As cost-effective functionals with improved general reliability are generated they can be tested against our CCSD(T)/CBS plus additional correction results. The calculations at the CCSD(T)/CBS level described here could be useful in the development of new exchange-correlation functionals that include more

(73) DeYonker, N. J.; Cundari, T. R.; Wilson, A. K. *J. Chem. Phys.* **2006**, *124*, 114104. DeYonker, N. J.; Grimes, T.; Yockel, S.; Dinescu, A.; Mintz, B.; Cundari, T. R.; Wilson, A. K. *J. Chem. Phys.* **2006**, *125*, 104111. DeYonker, N. J.; Peterson, K. A.; Steyl, G.; Wilson, A. K.; Cundari, T. R. *J. Phys. Chem. A* **2007**, *111*, 11269. DeYonker, N. J.; Williams, T. G.; Imel, A. E.; Cundari, T. R.; Wilson, A. K. *J. Chem. Phys.* **2009**, *131*, 024106.

(74) Curtiss, L. A.; Redfern, P. C.; Raghavachari, K.; Rassolov, V.; Pople, J. A. *J. Chem. Phys.* **1999**, *110*, 4703. Curtiss, L. A.; Raghavachari, K.; Redfern, P. C.; Rassolov, V.; Pople, J. A. *J. Chem. Phys.* **1998**, *109*, 7764. Curtiss, L. A.; Redfern, P. C.; Raghavachari, K. *J. Chem. Phys.* **2007**, *126*, 084108. Curtiss, L. A.; Redfern, P. C.; Raghavachari, K. *J. Chem. Phys.* **2007**, 126. Mayhall, N. J.; Raghavachari, K.; Redfern, P. C.; Curtiss, L. A. *J. Phys. Chem. A* **2009**, *113*, 5170.

transition metal compounds in their parametrization as there is a lack of good thermodynamic data on transition metal compounds.

A possible way to avoid the use of DFT for the larger substituents is to use the model chemistries such as ccCA[73] or the Gn (n = 3/4) series of composite methods[74] which have been expanded to transition metals. An issue with these methods, especially ccCA or the cost-efficient Gn(MP2) methods, is that the small basis set coupled cluster values are effectively extrapolated to the complete basis set limit using second order Møller−Plesset (MP2) theory. As long as MP2 is giving qualitatively reliable values, then these methods should work, but care must be taken that MP2 is providing a reasonable description of the wave function.

Conclusions

High level coupled cluster CCSD(T) calculations, extrapolated to the complete basis set limit, were used to evaluate the Group 10 transition metal $M-PH_3$ bond energies for the 0 and +2 oxidation states. The additional energy corrections can either increase or decrease the $M-PH_3$ BDE by up to 4 kcal/mol so they cannot be neglected. The M−P bond distance increases from Ni to Pd and then decreases slightly for Pt, and this trend is reflected in the values of the stretching frequencies. The higher oxidation state has the lower first BDE (reactions 2 and 4) with the two BDEs being comparable for Pd within 2 kcal/mol. The second BDE (reactions 1 and 3) is greater than the first for Pt and Pd, and the opposite holds for Ni in both oxidation states. A wide range of DFT exchange-correlation functionals were also evaluated to assess the performance of DFT. None of these functionals can be used to predict all of the $M-PH_3$ bond energies for M = Ni, Pd, Pt in the 0 or +2 oxidation states within even 5 kcal/mol. The best performing DFT functionals on average were the generalized gradient corrected PBE and PW91 functionals commonly used in periodic boundary condition calculations with plane waves.

Acknowledgment. This work was supported by the Chemical Sciences, Geosciences and Biosciences Division, Office of Basic Energy Sciences, U.S. Department of Energy (DOE) under Grant DE-FG02-03ER15481 (catalysis center program). D.A.D. also thanks the Robert Ramsay Chair Fund of The University of Alabama for support. Part of this work was performed at the W. R. Wiley Environmental Molecular Sciences Laboratory, a national scientific user facility sponsored by DOE's Office of Biological and Environmental Research and located at Pacific Northwest National Laboratory, operated for the DOE by Battelle.

Supporting Information Available: Figure of general catalytic cycle, T_1 diagnostics, $M-PH_3$ binding energies as a function of basis set, singlet−triplet energy splittings, metal-phosphine bond dissociation energies calculated with various exchange-correlation functionals and the aD-PP basis sets and deviations from the CCSD(T)/CBS calculated BDEs and optimized MPH_3, $M(PH_3)_2$, MPH_3Cl_2, $M(PH_3)_2Cl_2$, and MCl_2 XYZ coordinates at the B3LYP/aD-PP level. This material is available free of charge via the Internet at http://pubs.acs.org.